Journal of Bacteriology

Polyphosphate Storage during Sporulation in the Gram-Negative Bacterium Acetonema longum

Elitza I. Tocheva, Anne E. Dekas, Shawn E. McGlynn, Dylan Morris, Victoria J. Orphan and Grant J. Jensen

J. Bacteriol. **2013, 195(17):3940. DOI: 10.1128/JB.00712-13. Published Ahead of Print 28 June 2013.**

JB
Journals.ASM.org

Polyphosphate Storage during Sporulation in the Gram-Negative Bacterium *Acetonema longum*

Elitza I. Tocheva,[a] Anne E. Dekas,[c]* Shawn E. McGlynn,[c] Dylan Morris,[a] Victoria J. Orphan,[c] Grant J. Jensen[a,b]

Division of Biology,[a] Howard Hughes Medical Institute,[b] and Geological and Planetary Sciences,[c] California Institute of Technology, Pasadena, California, USA

Using electron cryotomography, we show that the Gram-negative sporulating bacterium *Acetonema longum* synthesizes high-density storage granules at the leading edges of engulfing membranes. The granules appear in the prespore and increase in size and number as engulfment proceeds. Typically, a cluster of 8 to 12 storage granules closely associates with the inner spore membrane and ultimately accounts for ~7% of the total volume in mature spores. Energy-dispersive X-ray spectroscopy (EDX) analyses show that the granules contain high levels of phosphorus, oxygen, and magnesium and therefore are likely composed of polyphosphate (poly-P). Unlike the Gram-positive *Bacilli* and *Clostridia*, *A. longum* spores retain their outer spore membrane upon germination. To explore the possibility that the granules in *A. longum* may be involved in this unique process, we imaged purified *Bacillus cereus*, *Bacillus thuringiensis*, *Bacillus subtilis*, and *Clostridium sporogenes* spores. Even though *B. cereus* and *B. thuringiensis* contain the *ppk* and *ppx* genes, none of the spores from Gram-positive bacteria had granules. We speculate that poly-P in *A. longum* may provide either the energy or phosphate metabolites needed for outgrowth while retaining an outer membrane.

Bacteria have the ability to store energy and nutrients such as carbon, phosphate, and nitrogen in the form of granules (1). Inorganic phosphorus (P_i) is stored in the form of polyphosphate (poly-P), chains of tens to hundreds of P_i residues, linked by high-energy phosphoanhydride bonds (2). A variety of roles for poly-P granules have been suggested in cell membrane formation, transcriptional and enzymatic regulation, stress and stationary-phase responses, and cation sequestration (3). Even though the mechanism underlying poly-P accumulation is not clearly understood, the principal enzymes involved in the metabolism of poly-P in bacteria have been identified: two classes of poly-P kinases (PPK1 and PPK2) polymerize the terminal phosphate of ATP onto a poly-P chain and can also work in reverse to generate ATP from poly-P, and exopolyphosphatase (PPX) hydrolyzes the terminal phosphate from linear poly-P (4). Genes encoding PPK are present in many bacteria, including various human pathogens (5). Deletion of *ppk* affects growth, motility, quorum sensing, biofilm formation, and virulence (4, 6, 7). In the opportunistic pathogen *Bacillus cereus*, the Δ*ppx* mutant was also impaired in sporulation (8).

Sporulation is a complex morphological process performed by some members of the phylum *Firmicutes* when nutrients are limited (9). The process begins with an asymmetric cell division, followed by the engulfment of the smaller compartment by the bigger, mother cell (10). At the end of sporulation, two membranes and numerous protective layers surround the mature spore. When the conditions are favorable again, the spore germinates and a new cell is released via outgrowth (10). Our previous studies on sporulation revealed that, unlike *Bacilli* and *Clostridia*, the noncanonical Gram-negative organism *A. longum* retains both spore membranes during outgrowth (11). Here, we describe how during sporulation, *Acetonema longum* also forms small dense bodies at the leading edges of engulfing membranes. The number and size of these bodies increase as engulfment proceeds, reaching a final number of 8 to 12 per mature spore. Using bioinformatics, nanoscale secondary ion mass spectrometry (NanoSIMS), electron cryotomography (ECT), and energy-dispersive X-ray spectroscopy (EDX), we identify these bodies as poly-P storage granules (SGs) and discuss their possible roles in sporulation.

MATERIALS AND METHODS

Sample preparation. *Acetonema longum* strain APO-1 cells were grown as described previously (12). Sporulating cells were harvested from cultures entering stationary phase. *Bacillus subtilis*, *B. cereus*, and *Bacillus thuringiensis* cells were grown in one-fourth Luria-Bertani medium (Life Technologies), and sporulation was induced by suspending exponential-phase cells in sporulation medium (13). One liter of sporulation medium contains 3 μM $FeCl_3 \cdot 6H_2O$, 40 mM $MgCl_2 \cdot 6H_2O$, 38 mM $MnCl_2 \cdot 4H_2O$, 0.01 M NH_4Cl, 75 mM Na_2SO_4, 0.12 M NH_4NO_3, 0.05 M KH_2PO_4, 0.25 mM morpholinepropanesulfonic acid (MOPS), pH 7.5, 0.02% glutamic acid, 0.1 mM $CaCl_2$, 4 mM $MgSO_4$. Pure spores from *A. longum*, *B. subtilis*, *B. cereus*, and *B. thuringiensis* were harvested by centrifugation and purified from mother cells as described previously (14). *Clostridium sporogenes* spores were a kind gift from Adrian Ponce. Cells and spores were grown and purified as described previously (15).

Electron cryotomography. Pure spores and cells were prepared for ECT by plunge freezing in nitrogen-cooled liquid ethane. Images and tilt-series were collected on an FEI Polara (FEI Company, Hillsboro, OR) 300-kV field emission gun (FEG) transmission electron microscope equipped with a Gatan energy filter and a lens-coupled 4k-by-4k UltraCam camera (Gatan, Pleasanton, CA) or a Titan Krios (FEI Company, Hillsboro, OR) microscope equipped with a Gatan energy filter and a K2 Summit direct detector (Gatan, Pleasanton, CA). Samples were imaged

Received 16 June 2013 Accepted 20 June 2013
Published ahead of print 28 June 2013
Address correspondence to Grant J. Jensen, Jensen@caltech.edu.
* Present address: Anne E. Dekas, Chemical Sciences Division, Lawrence Livermore National Laboratory, Livermore, California, USA.
Supplemental material for this article may be found at http://dx.doi.org/10.1128/JB.00712-13.

doi:10.1128/JB.00712-13

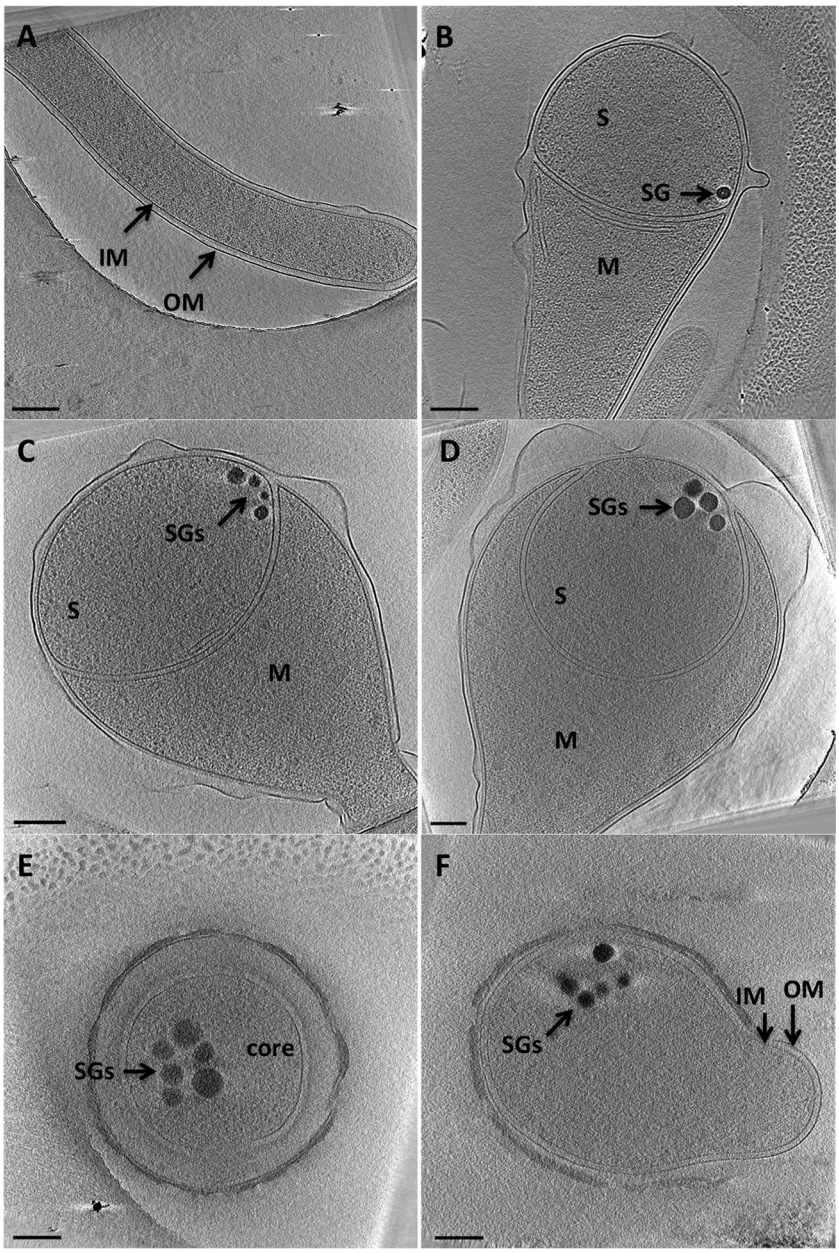

FIG 1 Storage granule formation during sporulation in *A. longum*. (A) Tomographic slices through vegetative cell; (B) sporulating cell during early stages of engulfment; (C and D) sporulating cell during later stages of engulfment; (E) mature spore; (F) germinating cell. Abbreviations: S, spore; M, mother cell; SG, storage granule; IM, inner membrane, OM, outer membrane. Bar, 200 nm.

with 200 $e^-/Å^2$, a defocus of −10 μm, and a tilt range from −60 to +60°. Three-dimensional reconstructions and segmentations were produced with IMOD (16).

Traditional electron microscopy (EM) of pure *A. longum* spores. Pure spores were chemically fixed based on protocols developed by Sabatini et al. (17). Briefly, primary fixation was done in 2.5% glutaraldehyde in buffer A (0.1 M sodium cacodylate buffer, pH 7.2). After three consecutive rinses in buffer A, the spores were fixed with 1% osmium tetroxide in buffer A. Epon epoxy resin was sequentially dissolved in 50%, 70%, and 100% and infiltrated into the spores. Once fully infiltrated, the resin was cured at 60°C for 2 days and then sectioned with an ultramicrotome. The thickness of the sections was 300 nm. Projection images were collected on a Tecnai T12 electron microscope.

NanoSIMS of *A. longum* spores. Sections were prepared as described above for traditional EM analysis. NanoSIMS analyses were performed using a Cameca nanoscale secondary ion mass spectrometry (NanoSIMS) 50L instrument (Gennevilliers, France). A primary Cs^+ ion beam was focused to an ~100-nm spot size and scanned over the sample in 256 by 256 pixel rasters to generate secondary ions. Dwell time was 1 to 5 ms per pixel, and raster size was 3 by 3 μm. Five secondary ions ($^{12}C^-$, $^{16}O_2{}^-$, $^{31}P^-$, $^{32}S^-$, and $^{14}N^{12}C^-$) were collected simultaneously using electron multipliers.

EDX analysis of whole *A. longum* spores. EDX analysis was performed on an FEI Titan 80- to 300-kV scanning transmission electron microscope equipped with an Oxford Instruments System Detector 7773 (FEI Company, Hillsboro, OR). Mature hydrated spores from *A. longum*

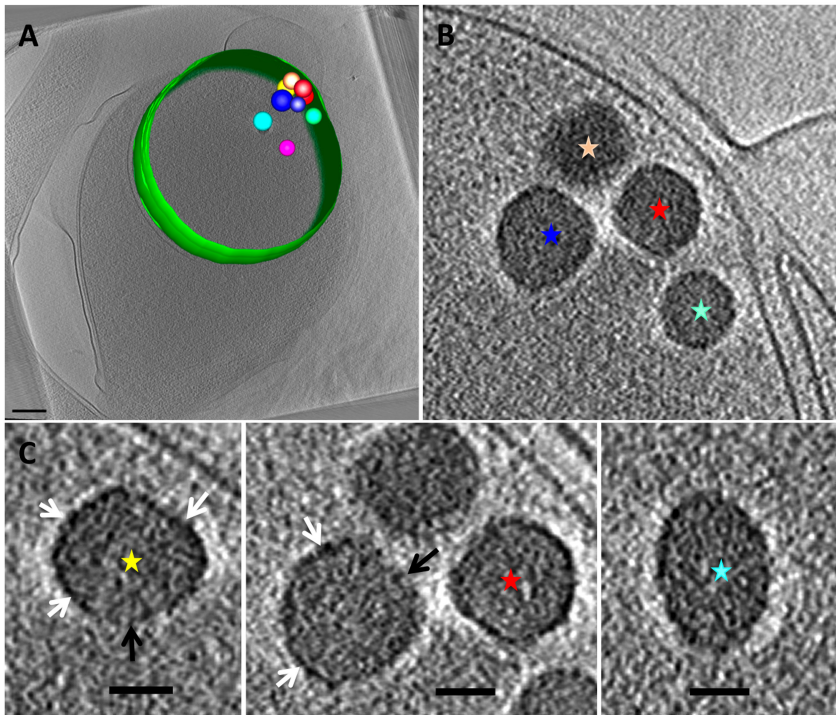

FIG 2 Structural features of the storage granules in *A. longum*. (A) Segmentation of the sporulating *A. longum* cell from Fig. 1D shows that 9 storage granules (represented as colored spheres) are clustered together and pressed against the inner spore membrane (green). Bar, 200 nm. (B) The storage granules are located close to the leading edge of the engulfing membrane. Colored stars correspond to the colors of the storage granules in panel A. (C) The granules exhibit a variety of roughly spherical shapes and are surrounded by a patchy surface layer. White arrows indicate areas of the presence of a proteinaceous layer; black arrows indicate the absence of a layer. Bar, 50 nm.

were placed on carbon-coated copper grids and air dried. The FEI transmission EM (TEM) imaging and analysis (TIA) software package was used to acquire data from a point measurement over a storage granule and from an area over a whole spore. EDX spectra of different areas were collected at 80 kV and a dosage of ~50 $e^{-}/Å^{2}$.

Homology searches. Several kinds of storage granules (SGs) have been described in bacteria, including glycogen, poly-β-hydroxybutyrate (PHB), polyphosphate, "sulfur-rich" granules, and "nitrogen-rich" granules (18–22). We searched for genes encoding enzymes associated with the production of storage granules in the genomes of *A. longum* and a number of "control" species, including *Ralstonia eutropha* (known to form PHB granules) (23), *Caulobacter crescentus* (known to form polyphosphate granules) (24), *Escherichia coli* (known to store glycogen) (25), and *Allochromatium vinosum* (known to form sulfur globules). The well-known endospore-forming species *B. subtilis* and *C. sporogenes* were also included as controls. To analyze the distribution of enzymes responsible for storage granule formation, we conducted BLAST searches of the several genomes using the blastp program with low-complexity filtering disabled and a strict E value threshold of 1e−10 (26). The query proteins used for these searches for glycogen storage were GlgBI (NP_629578.1) and GlgBII (NP_631386.1); those for PHB granules were PhaC (YP_726471.1), PhaP (YP_001171240.1), PhaZ1 (YP_725659.1), and PhaZ2 (YP_727307.1); those for polyphosphate storage were PPK1 (NP_416996.1) and PPX (NP_416997.1); and those for sulfur globules were SgpA (YP_003443861.1) and SgpB (YP_003442351.1).

Homology searches for just the poly-P enzymes in all sequenced sporulating bacteria were performed using the Pfam domains PF02503, PF03976, and PF02541 for PPK1, PPK2, and PPX, respectively.

RESULTS

ECT of sporulating *A. longum* cells reveals storage granules. As described in the work of Tocheva et al., cryotomograms of >250 *A. longum* cells were recorded at different stages of sporulation (11). Dense storage granules (SGs) were rarely observed (~1%) in vegetative cells of *A. longum* (Fig. 1A) but were consistently found in all prespores at the leading edges of engulfing membranes during early stages of engulfment (Fig. 1B). The number and size of the SGs increased as sporulation proceeded (Fig. 1C and D). Measurements of the distance of the SGs to the closest leading edge of engulfing membranes show a range of distances (from 67 nm to 272 nm), with the closest SG located 71 ± 7 nm from a leading edge. At the end of engulfment, all mature *A. longum* spores typically contained 8 to 12 storage granules with diameters of 40 to 120 nm, accounting for ~7% of the spore volume (Fig. 1E). In mature spores, the SGs remained clustered but were no longer proximal to the inner spore membrane. The SGs persisted throughout germination and outgrowth (Fig. 1F), though no specific localization with respect to the newly emerging cell was apparent.

Appearance of SGs. The SGs in *A. longum* appeared dense and grossly spherical, surrounded by an even denser shell (Fig. 2). Compared to other organisms, they closely resembled the size, density, and shape of the poly-P storage granules observed in *Caulobacter crescentus* and other organisms (see Fig. S4B in the supplemental material) (24). The shell around the SGs was discontinuous, only partially covering the granule (Fig. 2C; white arrows indicate the presence and black arrows indicate the absence of the protein layer). No patterns in the positions of the shell patches were recognized. In contrast to reports of an apparent membranous shell surrounding poly-P storage granules in *Agrobacterium*

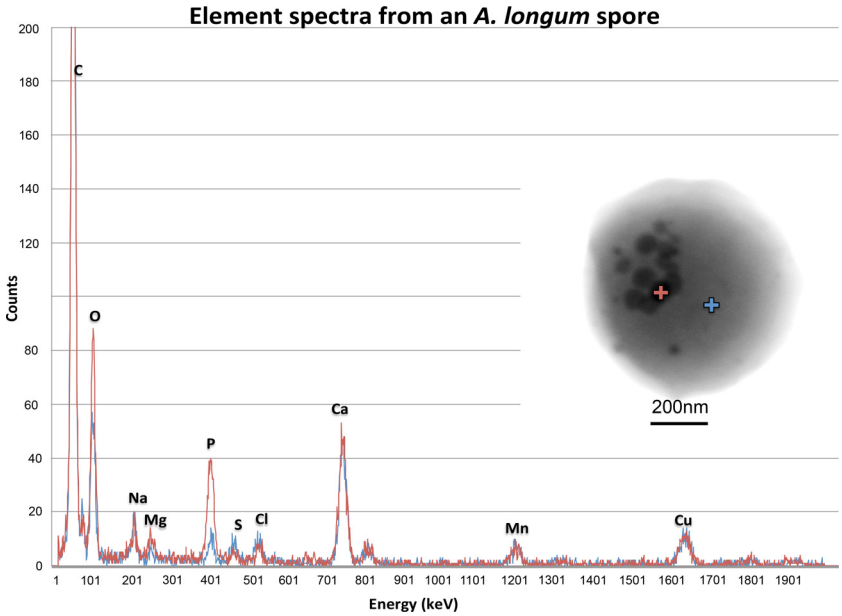

FIG 3 High-dose EDX point analysis of a storage granule. The elemental compositions within a storage granule and a random location outside the granule but within the spore core are shown in red and blue, respectively. Major peaks are assigned. Data show elevated levels of P, O, and Mg in the storage granule compared to the spore core. The inset shows a scanning-transmission EM image of the air-dried spore used for imaging, with crosses marking the positions analyzed.

tumefaciens and *Rhodospirillum rubrum* (27), the surrounding shell in *A. longum* was both discontinuous and variable in thickness and was therefore likely proteinaceous. The cores of the SGs appeared granular and void of internal organization. Fourier transforms of the images also failed to reveal internal order (data not shown).

Traditional EM of mature *A. longum* spores. Traditional EM methods failed to preserve the SG consistently (see Fig. S1 in the supplemental material). Using the same preparation method and sections, sometimes the SGs were retained, and other times they were lost, leaving "holes" in the section that are a well-known artifact of chemical fixation and alcohol dehydration (28). The inconsistency of SG preservation with traditional EM methods complicated elemental data acquisition, and precautions were therefore taken to analyze only dense (preserved) granules.

Mature spores from *Bacilli* and *Clostridia* lack SGs. In order to explore the role of poly-P SGs in sporulation in general, mature spores of other sporulating bacteria were also imaged with ECT. In contrast to *A. longum*, mature *B. subtilis*, *B. cereus*, *B. thuringiensis*, and *C. sporogenes* lacked dense SGs (see Fig. S2 in the supplemental material).

Elemental mapping of *A. longum* spores using NanoSIMS. To investigate the intracellular elemental distribution in a spore, thin sections of three *A. longum* spores were analyzed with nanoscale secondary ion mass spectrometry (NanoSIMS). Areas of increased phosphorus concentration were observed within the spores (see Fig. S3 in the supplemental material). Peaks were also visible in the $^{31}P^-/^{14}N^{12}C^-$ ratio image, in patterns different from those seen for the other elements (data not shown), demonstrating that they were not an artifact of sample topology or uneven generation of secondary ions (see Fig. S3C). Due to the lower sensitivity of NanoSIMS for phosphorus, the $^{31}P^-$ signal for DNA and RNA from the core of mature spores was not detected.

EDX. To further explore the elemental composition of the SGs, EDX was employed. *A. longum* spores and SGs were identified using scanning-transmission electron microscopy (Fig. 3). EDX spectra were then collected and showed elevated counts for O, P, and Mg but not Na, S, Cl, Ca, Mn, and Cu within SGs. The counts for phosphorus in the granules were ~3-fold greater than those for magnesium but half those for oxygen (Fig. 3). The copper and some of the carbon detected likely came from the EM grid. The distribution and overall shape of the storage granule cluster correlated well with elevated signals for P, O, and Mg ions in areal analyses (Fig. 4).

Bioinformatics. *A. longum* possesses the genes known to mediate storage of polyphosphate and glycogen but not sulfur or PHB (see Fig. S4A in the supplemental material). While PPK and PPX are present in some *Bacilli* (*B. cereus* and *B. thuringiensis*, also imaged with tomography), most *Clostridia* (for example, *C. sporogenes*) and some *Bacilli* (for example, *B. subtilis*) lacked the genes associated with poly-P formation. *A. longum* and *Pelosinus fermentans* were the only Gram-negative endospore-forming *Firmicutes* that had been sequenced, and both had *ppk* and *ppx* genes.

Volume calculations of SGs. To examine the fate of the SGs during germination and outgrowth, we performed volume calculations of the SGs in mature spores and germinating and outgrowing *A. longum* cells ($n = 25$) (Fig. 5). Our results show that while mature spores had clusters of SGs occupying ~5×10^6 nm^3, the volume and number of the SGs gradually decreased in germinating cells (cells with hydrolyzed cortex, Fig. 5C and D) to ~3.5×10^6 nm^3. The volume and number of SGs continued to decrease during initial stages of outgrowth (Fig. 5E and F) and were ultimately the lowest in cells at later stages of outgrowth (total volume of ~1.2×10^6 nm^3).

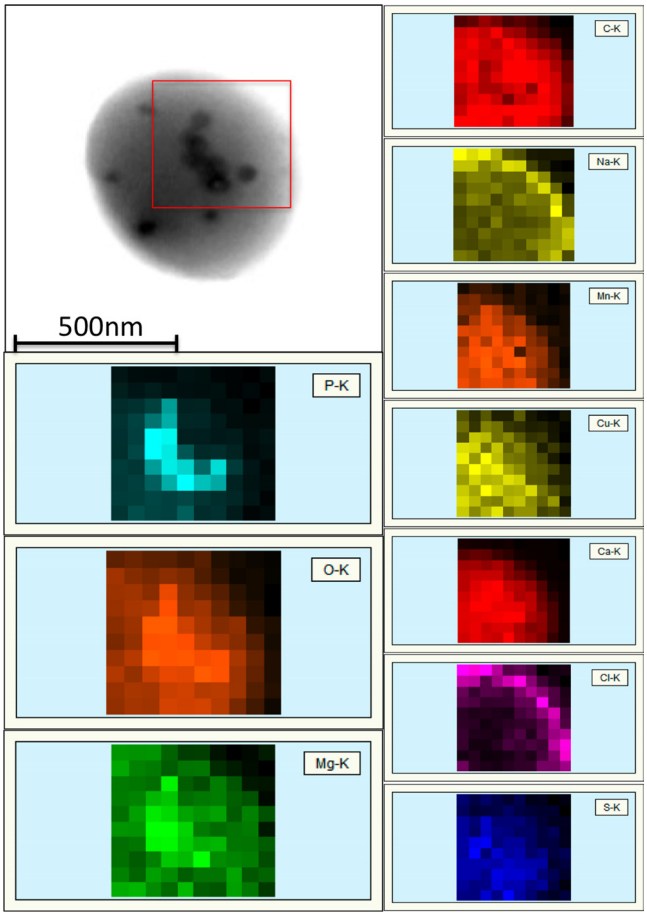

FIG 4 Lower-dose EDX area scan of a mature *A. longum* spore. Top left, scanning-transmission EM image of the spore. Other panels, individual element distributions within the scanned area. P, O, and Mg but not the other elements are seen to be higher inside the storage granules than outside. (The "K" in the panel titles corresponds to the atomic shell assessed for the X-ray dispersion.)

DISCUSSION

Here, we have called attention to our observation that *A. longum* spores contain highly dense storage granules. Following tomographic studies of sporulating cells, visual inspection and comparison to characterized SGs in other organisms suggested that the SGs observed in *A. longum* were enriched in phosphorus. EDX analyses of the SGs in mature spores showed high concentrations of phosphorus, oxygen, and Mg^{2+} indicative of concentrated phosphate. Traditional EM images, bioinformatics analyses, and NanoSIMS analysis support the conclusion that the granules are likely composed of poly-P. Further analysis needs to be performed to characterize the ratio and lengths of the phosphate chains in the SGs, and we do not exclude the possibility that carbon may be present in the granules as well. Previous studies have shown that phosphate concentrates into granules by polymerizing into long chains of polyanionic phosphate (29). Divalent cations have been previously shown to form ionic bonds between separate phosphate groups, allowing for denser packing (30). In the case of *A. longum*, the cation is likely Mg^{2+}, since Mg^{2+} levels in the granules were also elevated. The high concentration of poly-P excludes proteins and other organic carbon, thus explaining the slight dip observed in the carbon EDX counts within granules (Fig. 4).

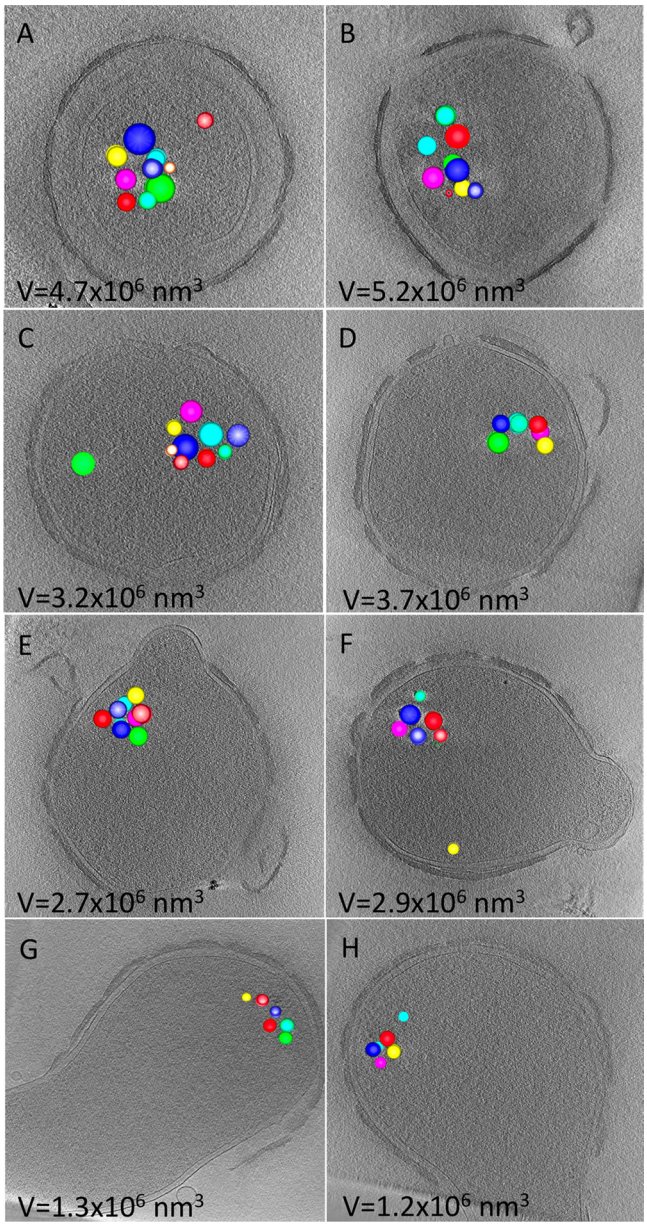

FIG 5 Volume calculations of the storage granules in mature spores and germinating and outgrowing *A. longum* cells. (A and B) Tomographic slices through mature spores. The storage granules are segmented and represented as spheres in different colors. (C and D) Spores that had hydrolyzed their cortex but maintained an intact spore coat. (E and F) Early stages of outgrowth. (G and H) Late stages of outgrowth. The total volume of the SGs is shown in each panel.

At this point, we can only speculate about the role of poly-P SGs in *A. longum* sporulation. Boutte et al. showed that poly-P appears to inhibit the swarmer-to-stalk transition in *Caulobacter* sp. under glucose exhaustion (31). Poly-P may play a similar regulatory role during sporulation in *A. longum*. Interestingly, previous work suggests that in the opportunistic pathogen *B. cereus*, poly-P depolymerization may induce or at least promote efficient sporulation in that organism (8). Alternatively, poly-P has been shown to be associated with the nucleoid and important for chromosomal packing or DNA segregation (32–34). Poly-P may there-

fore help pack and dehydrate the DNA in *A. longum* spores, but again, such a role would not be general, since spores of other species do not contain poly-P storage granules. The position of the storage granules at the leading edge of engulfing membranes may be a clue about their formation or use, but the significance remains unclear.

One obvious difference between *A. longum* and other endospore-forming bacteria, which may be relevant to its unique production of poly-P SGs, is the presence of an outer membrane. The basic topology of sporulation in all species produces two membranes, both of which originate from the cytoplasmic membrane of the mother cell and then later surround the mature spore (11, 35). When Gram-positive cells germinate, the second membrane dissociates together with the spore coat and is lost. In the case of Gram-negative sporulating bacteria like *A. longum*, the new outgrowing vegetative cell retains the second membrane (11). In addition, this second membrane is at some point transformed from an "inner" to an "outer" membrane. *A. longum* may therefore store poly-P in SGs as a source of energy or building blocks for its unique germination challenges. Toso et al. estimated that a 150-nm-diameter poly-P granule contains about 6.5×10^{-5} pmol of phosphate (36). Since mature *A. longum* spores contain approximately 10 100-nm-diameter poly-P granules, this is enough to produce an ATP concentration within the small spore nearly 100× that of a normal exponentially growing cell (~10 mM [37]). Considered another way, this is enough energy to approximately double the number of proteins in the spore (38) or synthesize enough fatty acids to cover 5× the area of both the inner and outer spore membranes. Volume calculations of SGs in mature *A. longum* spores and cells at different stages of germination and outgrowth support this hypothesis. Our observations show a consistent decrease in the size and number of the SGs from mature spores to later stages of outgrowth (Fig. 5), suggestive of the SGs being consumed during outgrowth. Furthermore, none of the Gram-positive spore-forming bacteria that we characterized here possess SGs in their mature spores.

Once *A. longum* becomes genetically tractable, mutation studies may help identify the role of poly-P. If sporulation efficiency is impaired in a Δ*ppk* mutant, for example, then accumulation of poly-P may be necessary for engulfment. If a Δ*ppx* mutant fails to germinate, however, then a role of poly-P in outgrowth could be considered.

ACKNOWLEDGMENTS

We acknowledge the use of electron microscopy facilities at the UCLA Electron Imaging Center for NanoMachines at the California NanoSystems Institute (CNSI) and thank Ivo Atanasov and Dan Taso for technical assistance with EDX data collection and analysis. We thank Yunbin Guan and John Eiler for assistance with the NanoSIMS measurements. We thank Adrian Ponce for providing the *C. sporogenes* spores.

The NanoSIMS apparatus is housed within the Caltech Microanalysis Center and is partially funded by the Gordon and Betty Moore Foundation. This work was funded in part by the Howard Hughes Medical Institute, the Caltech Center for Environmental Microbial Interactions, and gifts to Caltech from the Gordon and Betty Moore Foundation.

This work was partially performed under the auspices of the U.S. Department of Energy by Lawrence Livermore National Laboratory under contract DE-AC52-07NA27344.

REFERENCES

1. **Shively JM.** 1974. Inclusion bodies of prokaryotes. Annu. Rev. Microbiol. **28:**167–187.
2. **Brown MR, Kornberg A.** 2004. Inorganic polyphosphate in the origin and survival of species. Proc. Natl. Acad. Sci. U. S. A. **101:**16085–16087.
3. **Kornberg A, Rao NN, Ault-Riche D.** 1999. Inorganic polyphosphate: a molecule of many functions. Annu. Rev. Biochem. **68:**89–125.
4. **Rao NN, Kornberg A.** 1999. Inorganic polyphosphate regulates responses of *Escherichia coli* to nutritional stringencies, environmental stresses and survival in the stationary phase. Prog. Mol. Subcell. Biol. **23:**183–195.
5. **Zhang H, Gomez-Garcia MR, Shi X, Rao NN, Kornberg A.** 2007. Polyphosphate kinase 1, a conserved bacterial enzyme, in a eukaryote, Dictyostelium discoideum, with a role in cytokinesis. Proc. Natl. Acad. Sci. U. S. A. **104:**16486–16491.
6. **Ault-Riche D, Fraley CD, Tzeng CM, Kornberg A.** 1998. Novel assay reveals multiple pathways regulating stress-induced accumulations of inorganic polyphosphate in *Escherichia coli*. J. Bacteriol. **180:**1841–1847.
7. **Rashid MH, Rumbaugh K, Passador L, Davies DG, Hamood AN, Iglewski BH, Kornberg A.** 2000. Polyphosphate kinase is essential for biofilm development, quorum sensing, and virulence of *Pseudomonas aeruginosa*. Proc. Natl. Acad. Sci. U. S. A. **97:**9636–9641.
8. **Shi X, Rao NN, Kornberg A.** 2004. Inorganic polyphosphate in *Bacillus cereus*: motility, biofilm formation, and sporulation. Proc. Natl. Acad. Sci. U. S. A. **101:**17061–17065.
9. **Piggot PJ, Hilbert DW.** 2004. Sporulation of *Bacillus subtilis*. Curr. Opin. Microbiol. **7:**579–586.
10. **Errington J.** 1993. *Bacillus subtilis* sporulation: regulation of gene expression and control of morphogenesis. Microbiol. Rev. **57:**1–33.
11. **Tocheva EI, Matson EG, Morris DM, Moussavi F, Leadbetter JR, Jensen GJ.** 2011. Peptidoglycan remodeling and conversion of an inner membrane into an outer membrane during sporulation. Cell **146:**799–812.
12. **Kane MD, Breznak JA.** 1991. *Acetonema longum* gen. nov. sp. nov., an H_2/CO_2 acetogenic bacterium from the termite, *Pterotermes occidentis*. Arch. Microbiol. **156:**91–98.
13. **Sterlini JM, Mandelstam J.** 1969. Commitment to sporulation in *Bacillus subtilis* and its relationship to development of actinomycin resistance. Biochem. J. **113:**29–37.
14. **Nicholson WL, Setlow P.** 1990. Dramatic increase in negative superhelicity of plasmid DNA in the forespore compartment of sporulating cells of *Bacillus subtilis*. J. Bacteriol. **172:**7–14.
15. **Yang W.** 2010. Fast viability assessment of *Clostridium* spores—survival in extreme environments. California Institute of Technology, Pasadena, CA.
16. **Kremer JR, Mastronarde DN, McIntosh JR.** 1996. Computer visualization of three-dimensional image data using IMOD. J. Struct. Biol. **116:**71–76.
17. **Sabatini DD, Bensch K, Barrnett RJ.** 1963. Cytochemistry and electron microscopy. The preservation of cellular ultrastructure and enzymatic activity by aldehyde fixation. J. Cell Biol. **17:**19–58.
18. **Brune DC.** 1995. Isolation and characterization of sulfur globule proteins from *Chromatium vinosum* and *Thiocapsa roseopersicina*. Arch. Microbiol. **163:**391–399.
19. **Shiba T, Tsutsumi K, Ishige K, Noguchi T.** 2000. Inorganic polyphosphate and polyphosphate kinase: their novel biological functions and applications. Biochemistry (Mosc.) **65:**315–323.
20. **Kadouri D, Jurkevitch E, Okon Y, Castro-Sowinski S.** 2005. Ecological and agricultural significance of bacterial polyhydroxyalkanoates. Crit. Rev. Microbiol. **31:**55–67.
21. **Yeo M, Chater K.** 2005. The interplay of glycogen metabolism and differentiation provides an insight into the developmental biology of *Streptomyces coelicolor*. Microbiology **151:**855–861.
22. **Obst M, Krug A, Luftmann H, Steinbuchel A.** 2005. Degradation of cyanophycin by *Sedimentibacter hongkongensis* strain KI and *Citrobacter amalonaticus* strain G isolated from an anaerobic bacterial consortium. Appl. Environ. Microbiol. **71:**3642–3652.
23. **Jendrossek D.** 2009. Polyhydroxyalkanoate granules are complex subcellular organelles (carbonosomes). J. Bacteriol. **191:**3195–3202.
24. **Comolli LR, Kundmann M, Downing KH.** 2006. Characterization of intact subcellular bodies in whole bacteria by cryo-electron tomography and spectroscopic imaging. J. Microsc. **223:**40–52.
25. **Leduc M, Frehel C, Siegel E, Van Heijenoort J.** 1989. Multilayered distribution of peptidoglycan in the periplasmic space of *Escherichia coli*. J. Gen. Microbiol. **135:**1243–1254.
26. **Altschul SF, Gish W, Miller W, Myers EW, Lipman DJ.** 1990. Basic local alignment search tool. J. Mol. Biol. **215:**403–410.
27. **Seufferheld M, Lea CR, Vieira M, Oldfield E, Docampo R.** 2004. The

H(+)-pyrophosphatase of Rhodospirillum rubrum is predominantly located in polyphosphate-rich acidocalcisomes. J. Biol. Chem. **279:**51193–51202.
28. **Dubochet J, Sartori Blanc N.** 2001. The cell in absence of aggregation artifacts. Micron **32:**91–99.
29. **Kulaev I, Vagabov V, Kulakovskaya T.** 1999. New aspects of inorganic polyphosphate metabolism and function. J. Biosci. Bioeng. **88:**111–129.
30. **Parsons AJ, Ahmed I, Rudd CD, Cuello GJ, Pellegrini E, Richard D, Johnson MR.** 2010. Neutron scattering and ab initio molecular dynamics study of cross-linking in biomedical phosphate glasses. J. Phys. Condens. Matter **22:**485403. doi:10.1088/0953-8984/22/48/485403.
31. **Boutte CC, Henry JT, Crosson S.** 2012. ppGpp and polyphosphate modulate cell cycle progression in *Caulobacter crescentus*. J. Bacteriol. **194:**28–35.
32. **Kahng LS, Shapiro L.** 2003. Polar localization of replicon origins in the multipartite genomes of *Agrobacterium tumefaciens* and *Sinorhizobium meliloti*. J. Bacteriol. **185:**3384–3391.
33. **Fraley CD, Rashid MH, Lee SS, Gottschalk R, Harrison J, Wood PJ, Brown MR, Kornberg A.** 2007. A polyphosphate kinase 1 (ppk1) mutant of *Pseudomonas aeruginosa* exhibits multiple ultrastructural and functional defects. Proc. Natl. Acad. Sci. U. S. A. **104:**3526–3531.
34. **Butan C, Hartnell LM, Fenton AK, Bliss D, Sockett RE, Subramaniam S, Milne JL.** 2011. Spiral architecture of the nucleoid in *Bdellovibrio bacteriovorus*. J. Bacteriol. **193:**1341–1350.
35. **Tocheva EI, Lopez-Garrido J, Hughes HV, Fredlund J, Kuru E, Vannieuwenhze MS, Brun YV, Pogliano K, Jensen GJ.** 2013. Peptidoglycan transformations during *Bacillus subtilis* sporulation. Mol. Microbiol. **88:**673–686.
36. **Toso DB, Henstra AM, Gunsalus RP, Zhou ZH.** 2011. Structural, mass and elemental analyses of storage granules in methanogenic archaeal cells. Environ. Microbiol. **13:**2587–2599.
37. **Bennett BD, Kimball EH, Gao M, Osterhout R, Van Dien SJ, Rabinowitz JD.** 2009. Absolute metabolite concentrations and implied enzyme active site occupancy in *Escherichia coli*. Nat. Chem. Biol. **5:**593–599.
38. **Piques M, Schulze WX, Hohne M, Usadel B, Gibon Y, Rohwer J, Stitt M.** 2009. Ribosome and transcript copy numbers, polysome occupancy and enzyme dynamics in Arabidopsis. Mol. Syst. Biol. **5:**314. doi:10.1038/msb.2009.68.